# Ice nucleation on surrogates of boreal forest SOA particles: effect of water content and oxidative age

**Ana A. Piedehierro**[1]**, André Welti**[1]**, Angela Buchholz**[2]**, Kimmo Korhonen**[2]**, Iida Pullinen**[2]**, Ilkka Summanen**[2]**, Annele Virtanen**[2]**, and Ari Laaksonen**[1,2]

[1]Finnish Meteorological Institute, Helsinki, Finland.
[2]Department of Applied Physics, University of Eastern Finland, Kuopio, Finland.

*Correspondence to:* Ana A. Piedehierro (ana.alvarez.piedehierro@fmi.fi)

**Abstract.** We investigate the effect of water content and oxidative age on ice nucleation using $100\,\mathrm{nm}$ monodisperse particles of boreal forest SOA surrogates. Ice nucleation experiments are conducted in the temperature range between $210$ and $240\,\mathrm{K}$ and from ice to water saturation using the Spectrometer for Ice Nuclei (SPIN). The effect of the particle water content on the ice nucleation process is tested by preconditioning $\alpha$-pinene SOA at different humidity (40%, 10% and <1% $RH_W$). The influence of the particle oxidative age is tested by varying their O:C ratio (oxygen-to-carbon ratios, O:C $\sim$ 0.45, 0.8, 1.1). To assess the suitability of $\alpha$-pinene as a model compound to study the ice nucleation properties of boreal forest SOA and to confirm the atmospheric relevance of our findings, we compare them to measurements of SOA using pine-needle oil or Scots pine tree emissions as precursors.

The ice nucleation measurements show that surrogates of boreal forest SOA particles promote only homogeneous ice formation. An effect of preconditioning humidity on homogeneous ice nucleation could be observed. Contrary to the expected behavior, homogeneous freezing is suppressed for SOA particles with high water content (preconditioned at 40% $RH_W$) and was only observed for SOA preconditioned at low $RH_W$ ($\leq$ 10%). No dependence of homogeneous freezing on the SOA oxidative age was observed. The results can be explained by a significant change of particulate water diffusivity as a function of humidity (from 10% to 40% $RH_W$) at $293\,\mathrm{K}$, where the aerosol is preconditioned. The measurements suggest that at low temperatures, water diffusion into dry SOA particles is slow enough to form a core-shell morphology. The liquid outer layer can equilibrate within the timescale of the experiment and freeze homogeneously. On SOA particles with higher water content, water diffuses faster into the particle, delaying equilibration at the particle surface and preventing the formation of a diluted shell, which can delay homogeneous freezing. We propose that the partial water vapor pressure to which the particles are exposed prior to an experiment can serve as an indicator of whether a core-shell structure is developing.

## 1 Introduction

Heterogeneous ice formation by ice nucleating particles (INP) allows the formation of cirrus clouds at lower humidity than required for ice formation by homogeneous freezing of solution droplets, which is determined by the water activity criterion (Koop et al., 2000). Typical cirrus cloud INPs are water insoluble particles such as mineral dusts, fly ash, metallic particles (DeMott et al., 2003; Cziczo et al., 2013) or soot (Bond et al., 2013). Prompted by the realization that secondary organic aerosol (SOA) particles can exist in a highly viscous, (semi-) solid state (Zobrist et al., 2008; Virtanen et al., 2010), the possibility that SOA particles could act as INPs has been investigated in the recent years (Möhler et al., 2008; Prenni et al., 2009; Wang et al., 2012; Ladino et al., 2014; Schill et al., 2014; Ignatius et al., 2016; Charnawskas et al., 2017; Wagner et al., 2017; Bertozzi et al., 2021). SOA acting as INPs affect precipitation formation, cloud cover and the cloud albedo. A better understanding of ice nucleation on SOA is of special relevance for predicting cloud properties in areas with boreal forest, where biogenic SOA can form in high concentrations. SOA particles are composed of oxidation products of volatile organic compounds (VOC), some of which are water soluble. In contrast to low viscosity (more liquid-like) particles, highly viscous aerosol are slow to take

up or lose water or other vapors in response to variations in gas-phase composition (Mikhailov et al., 2009; Koop et al., 2011; Shiraiwa et al., 2013; Yli-Juuti et al., 2017). This resistance is particularly pronounced under dry conditions or low temperatures where SOA particles can exist in a highly viscous, or glassy state (Koop et al., 2011; Virtanen et al., 2010; Zobrist et al., 2008).

Upon updraft-driven humidification in the atmosphere, (semi-) solid amorphous organic aerosol could act as INP in several ice nucleation mechanisms (Knopf et al., 2018). SOA particles that remain glassy during humidification could trigger ice formation via deposition nucleation (Murray et al., 2010). Upon humidification beyond the amorphous deliquescence relative humidity, water diffusion might be slow enough to form core-shell morphologies in particles with a highly viscous glassy matrix, allowing ice formation via immersion freezing (Berkemeier et al., 2014; Lienhard et al., 2015). This situation could take place during fast updrafts ($> 3 \, \mathrm{m \, s^{-1}}$) in which the equilibration time with the surrounding humidity is limited (Lienhard et al., 2015; Price et al., 2015). Typical equilibration times for $100 \, \mathrm{nm}$ $\alpha$-pinene SOA particles range from hours at $220 \, \mathrm{K}$ to minutes at $230 \, \mathrm{K}$ (Price et al., 2015). Continued humidification of the organic particles leads to complete liquefaction and homogeneous freezing as the only possible ice formation mechanism (Koop et al., 2011).

Previous studies have found that the ice nucleation (IN) ability of SOA particles varies between species: naphthalene-derived (Wang et al., 2012), methylglyoxal with methylamine (Schill et al., 2014) and isoprene-derived SOA particles (Wolf et al., 2020) were classified as effective INP, exhibiting ice formation onsets at humidities clearly below homogeneous freezing conditions. $\alpha$-pinene SOA was indicated to be ineffective at nucleating ice heterogeneously (e.g. Charnawskas et al., 2017, and references therein), while Ignatius et al. (2016) found $\alpha$-pinene SOA particles to be effective INPs in the deposition mode. Although the rapid cooling of the aerosol during most experiments could result in the development of a core-shell morphology, none of the above studies observed ice formation by immersion freezing.

Using a cloud particle model capable of simulating water diffusion in individual aerosol particles, Fowler et al. (2020) have recently shown that at temperatures between 200 and $220 \, \mathrm{K}$ a water layer condenses on $\alpha$-pinene SOA particles, which can freeze homogeneously. In accordance with laboratory studies showing only homogeneous ice formation of $\alpha$-pinene SOA particles, the same model indicates that at higher temperatures, water diffuses into particles, and freezing only takes place at humidities high enough to enable the freezing of solution droplets. Mie resonance measurements in levitating, highly viscous aerosol particles show steep gradients in water content between the core and outer layer (Bastelberger et al., 2018) supporting the interpretation that viscous SOA can adopt a core-shell structure, where the outer layer can freeze homogeneously.

We present experimental results of ice formation of atmospherically relevant surrogates of SOA particles, generated from biogenic emissions characteristic of boreal environments. To test the effect of water content and core-shell formation, $\alpha$-pinene SOA particles with different diffusivity are generated by varying the oxidative ageing and exposure of particles to different levels of humidity prior to cooling. The atmospheric relevance of the ice nucleation results from the $\alpha$-pinene SOA is confirmed by comparing to experiments with SOA particles formed from natural, boreal forest VOC.

## 2 Methods

The SOA Ice Nucleation Experiment (SINE) campaign was carried out at the University of Eastern Finland Aerosol Physics Laboratory in June - July 2019. The experiments focused on studying the IN efficiency of SOA formed from boreal forest emissions and the influence of particle water content and oxidation level on IN activity.

### 2.1 General experimental setup

A schematic of the experimental setup is depicted in Fig. 1. SOA was generated either in an atmospheric simulation chamber (ASC; Faiola et al. (2019); batch chamber) or a potential aerosol mass reactor (PAM; Aerodyne Research Inc.; Kang et al. (2007), Lambe et al. (2011); oxidative flow reactor). The details of the two SOA formation procedures are described in sections 2.2.1 and 2.2.2.

The SOA precursor concentrations (VOC, Tab. 1) were monitored by a high-resolution time-of-flight proton transfer reaction mass spectrometer (PTR-MS, Ionicon model 8000). The size distribution and the oxidative age (O:C ratio, Tab. 1) of the SOA particles were monitored using a scanning mobility particle sizer (SMPS: TSI, Inc. model DMA 3082, CPC 3775) and a high-resolution time-of-flight aerosol mass spectrometer (HR-AMS: Aerodyne Research Inc., DeCarlo et al., 2006), respectively. For the ice nucleation measurements with a spectrometer for ice nuclei (SPIN; Droplet Measurement Technologies) the aerosol was size-selected using a differential mobility analyzer (DMA; TSI, model 3082) and preconditioned at 40%, 10% or <1% RH$_\mathrm{W}$.

### 2.2 Aerosol generation

#### 2.2.1 $\alpha$-pinene SOA with different O:C generated with the PAM reactor

We used a PAM reactor to form $\alpha$-pinene SOA particles of different oxidative ages, characterized by their O:C ratio. A syringe pump (Nexus 3000, Chemyx Inc.) was used to create a constant injection of $\alpha$-pinene into a nitrogen carrier gas flow heated to $60 \, \mathrm{°C}$, which was introduced into the PAM reactor. In the PAM reactor, particles are formed by a) dry ozonolysis, b) wet ozonolysis, or c) wet photooxidation with
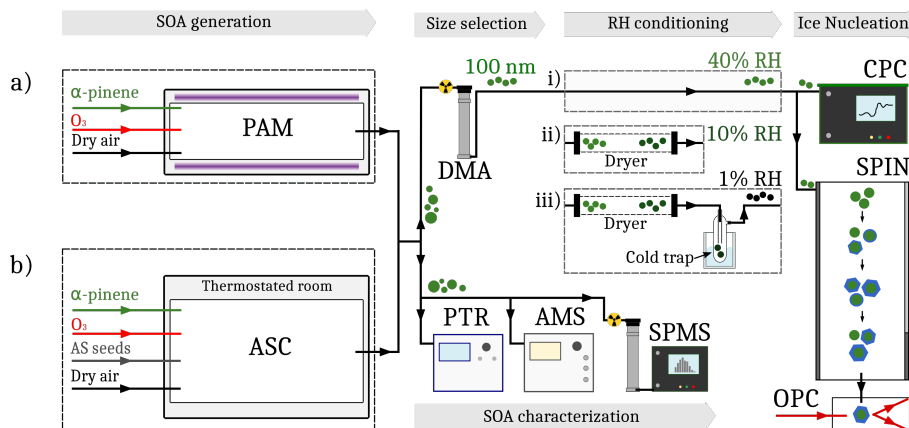
**Figure 1.** Experimental set-up during SINE. The set-up consists of five stages: SOA generation, size selection, SOA characterization, RH conditioning, and ice nucleation measurement. Two methods of SOA generation were used: a) homogeneous nucleation inside the PAM reactor and b) seeded nucleation inside the ASC. For the PAM experiments, three configurations of the RH conditioning stage were used before measuring the IN activity of the SOA particles: i) 40%, ii) 10% or iii) <1% $RH_W$).

OH radicals. The $O_3$ concentration, and in the photooxidation experiments the irradiation level, were adjusted to create SOA particles with a specific O:C ratio (see Tab. 1 for settings). Low-O:C SOA (O:C ~0.45) was produced in wet and dry ozonolysis experiments (#1 - #7). The photooxidation experiments (#8 - #12) generated medium- (O:C ~0.9) and high-O:C (O:C ~1.1) SOA. For dry ozonolysis, dry nitrogen and oxygen were used as carrier gases resulting in $RH_W$ of <2% in the sample flow exiting the PAM reactor. For wet ozonolysis and photooxidation experiments, the nitrogen flow was humidified to create $RH_W$ between 40% and 50% inside the reactor. The OH radicals in the photooxidation experiments were created from the photolysis of $O_3$ at 254 nm and consecutive reaction of the formed $O(^1D)$ with water vapor. Typical $O_3$ concentration was 6.5 - 7 ppm at the inlet of PAM. The average OH concentration inside the PAM reactor was 5 - 10 $\times10^8$ molec cm$^{-3}$ (estimated from OH exposure, Peng et al., 2015). The composition of the SOA particles formed in the PAM reactor were held constant over the course of the 4-5 hours needed for the IN measurements. Between two experiments, the PAM reactor and all connected tubes were flushed with nitrogen or purified air (custom-built system, dry compressed air followed by particle, active charcoal and potassium permanganate filters) for several hours. Before a new experiment started, the PAM reactor ran for at least 30 min at similar $O_3$ concentrations and irradiation as during the experiment but without VOC to ensure low levels of background SOA (< 1 $\mu$g m$^{-3}$).

### 2.2.2 Boreal forest surrogate SOA from ASC

A second set of experiments was conducted utilizing the 12 m$^3$ collapsible PTFE ASC to form SOA under atmospheric conditions (see Fig. 1). Aqueous ammonium sulfate particles were generated with an atomizer (Aerosol Genera-

tor Model 3076, TSI), subsequently dried below their efflorescence point in a silica gel dryer (50 cm long, outlet $RH_W$ < 15%) and injected into the ASC to reach seed concentrations of 5.0 – 7.5 $\times10^4$ cm$^{-3}$ at the start of VOC ozonolysis. For experiments #13 and #15, $\alpha$-pinene or pine needle oil were injected with a microliter syringe directly into a carrier gas flow. The injection times were adjusted to reach the desired 5 - 50 ppb in the ASC. The emissions from six 10 year-old pine saplings had been collected onto stainless steel multibed adsorbent cartridges containing Tenax TA and Carbograph adsorbent (Markes International, Inc.) during the springtime of 2019 (similar procedure as described by Faiola et al., 2019). For experiment #14, 4 of these tubes (equivalent to 30 h of emissions) were introduced into the ASC by flushing the cartridges with nitrogen for 20 min, while they were heated to 473 K. Mixing in the ASC was achieved by an additional flow of purified compressed air (> 50 L min$^{-1}$). $O_3$ was added to the chamber from a custom-built ozone generator, immediately afterwards, to start the ozonolysis reactions.

The precursor concentration in the ASC was monitored with the PTR-MS. The particle size and composition were monitored continuously with the SMPS and the HR-AMS. The IN measurements started after the maximum in the SOA mass concentration was reached, ensuring a constant particle composition during the IN measurements. Between experiments, the ASC was flushed for several hours with purified compressed air. Additionally, chemical cleaning was conducted by filling the ASC with high concentrations of $O_3$ (>500 ppb) for 30 – 60 min. These chemical cleaning intervals were followed by at least 10 h of flushing.

### 2.3 Ice nucleation measurements

The ice nucleation ability of 100 nm SOA particles was measured with the SPIN instrument (Garimella et al., 2016).

**Table 1.** Range of SOA formation and preconditioning parameters for each PAM reactor and ASC experiment. The VOC concentrations [VOC] reported for PAM experiments correspond to average concentrations while for ASC refer to starting concentrations. The variability of parameters during individual experiments were $RH_W \pm 1\%$, [VOC] $\pm 7.0$ ppb and O:C ratio $\pm 0.03$.

| Exp # | Reactor | VOC | [VOC] [ppb] | Formation $RH_W$ [%] | Dominant oxidant | O:C ratio | Seed | Preconditioning $RH_W$ [%] | Fig. |
|---|---|---|---|---|---|---|---|---|---|
| 1 | PAM | $\alpha$-pinene | 99 | 47 | $O_3$ | 0.46 | - | 40 | 2.a |
| 2 | PAM | $\alpha$-pinene | 131 | 40 | $O_3$ | 0.45 | - | <10 | 2.b |
| 3 | PAM | $\alpha$-pinene | 127 | 50 | $O_3$ | 0.44 | - | <10 | 2.b |
| 4 | PAM | $\alpha$-pinene | 137 | 50 | $O_3$ | 0.45 | - | <1 | 2.c |
| 5 | PAM | $\alpha$-pinene | 129 | 40 | $O_3$ | 0.45 | - | <1 | 2.c |
| 6 | PAM | $\alpha$-pinene | 122 | 2 | $O_3$ | 0.45 | - | <2 | 2.c |
| 7 | PAM | $\alpha$-pinene | 90 | 1 | $O_3$ | 0.46 | - | <1 | 2.c |
| 8 | PAM | $\alpha$-pinene | 105 | 44 | OH | 0.91 | - | 40 | 2.d |
| 9 | PAM | $\alpha$-pinene | 95 | 43 | OH | 0.88 | - | <10 | 2.e |
| 10 | PAM | $\alpha$-pinene | 98 | 44 | OH | 0.86 | - | <1 | 2.f |
| 11 | PAM | $\alpha$-pinene | 120 | 40 | OH | 1.05 | - | 40 | 2.g |
| 12 | PAM | $\alpha$-pinene | 107 | 42 | OH | 1.16 | - | <10 | 2.h |
| 13 | ASC | pine-needle-oil | 21 * | <15 | $O_3$ | 0.6 | $(NH_4)_2SO_4$ | <10 | 5.a |
| 14 | ASC | pine emissions | 6 * | <15 | $O_3$ | 0.53 | $(NH_4)_2SO_4$ | <10 | 5.b |
| 15 | ASC | $\alpha$-pinene | 6 * | <15 | $O_3$ | 0.61 | $(NH_4)_2SO_4$ | <10 | 5.c |

* concentration of VOCs detectable with PTR-MS

SPIN is a parallel plate, continuous flow diffusion chamber (CFDC). The specific instrument (SPIN5) used in this study has been modified to perform low temperature experiments (Welti et al., 2020). Inside the SPIN chamber, particles are exposed to RH- and T-conditions (temperature range 210 - 240 K and from ice to water saturation) relevant for ice formation in cirrus clouds. Ice formation during a residence time of 10 s is detected with an optical particle counter (OPC, details in Garimella et al., 2016). The ratio of ice forming particles, measured with the OPC and the number of particles introduced into SPIN, measured with a condensation particle counter (CPC; Airmodus A20), is reported as activated fraction (AF). The activated fraction is measured along RH scans at several temperatures. The evaporation section at the end of the chamber guarantees that droplets are not counted as ice with the OPC. In this study, the size-selected SOA particles were exposed to different humidity conditions before entering the SPIN, to probe the effects of particle water content on IN activity. The samples were introduced a) directly into the SPIN, b) through a silica gel diffusion dryer, or c) sequentially through a silica gel diffusion dryer and a liquid nitrogen cold trap (see Fig. 1). The preconditioning led to sample $RH_W$ at the SPIN inlet (Vaisala HMP110 humidity sensor) of 40%, 10%, or <1%, respectively. Later, we refer to these precondition settings as wet, dry and super dry.

## 3 Results and Discussion

### 3.1 Effect of O:C ratio and water content on ice formation conditions

The effects of oxidative age (approximated by the O:C ratio) and water content of $\alpha$-pinene SOA particles on ice formation were investigated. Note, that the water content of the particles was preconditioned after generation and before measuring their ice nucleation ability with the SPIN. The AF-spectra of $\alpha$-pinene SOA particles generated with different O:C and preconditioned at different humidity are shown in Fig. 2.

The O:C ratio appears to have a minor impact on the conditions of ice formation of the $\alpha$-pinene SOA particles. Schill and Tolbert (2012) reported that the O:C ratio of organic acids affects heterogeneous ice nucleation and suggested that this could also be the case for $\alpha$-pinene SOA. Aged particles (higher O:C ratio) would nucleate ice at lower humidity due to higher surface hydrophilicity, allowing the adsorption of an ice-like layer from which the ice phase can develop. The decrease in ice formation onset humidity was strongest for $0.3 < O:C < 0.5$ (Schill and Tolbert, 2012). In the range of O:C ratios covered here (0.45-1.1) no pronounced change in ice formation humidity was observed. Fig. 3 summarizes RH-conditions where AF = 1% were reached in dependence of O:C ratios. The humidity needed to reach 1% AF is close to humidities at which ammonium sulfate solution droplets freeze homogeneously (e.g. reported in Welti et al., 2020). This suggests that homogeneous freezing dominated the ice
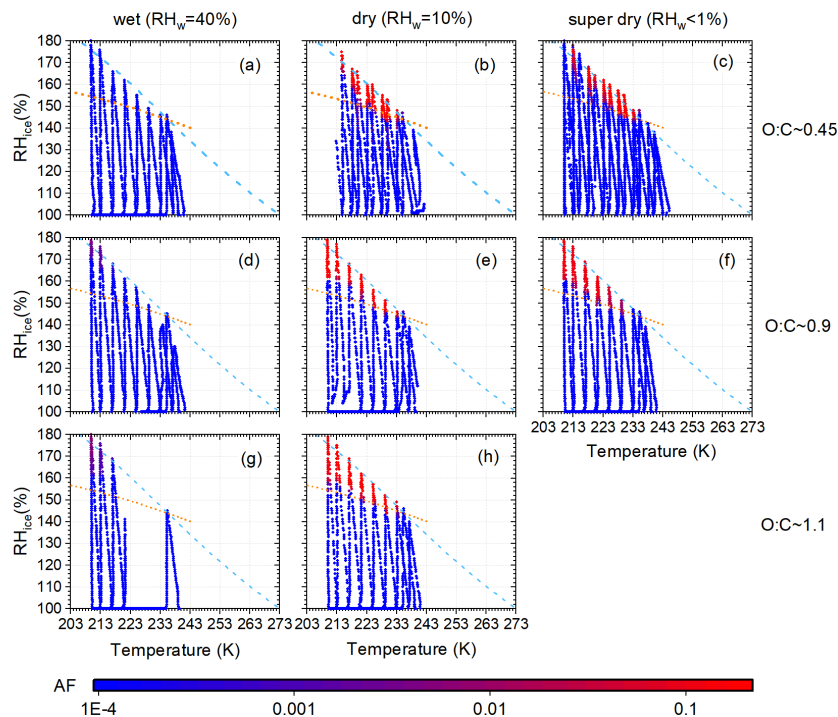
**Figure 2.** AF measurements for $\alpha$-pinene O:C $\sim$0.45, 0.9 and 1.1 (top, middle and bottom row) and 40%, 10%, <1% $RH_W$ (left, middle and right column). The color code indicates activated fraction. The dashed, light blue line marks water saturation. Conditions of homogeneous freezing (AF=1%) of $\alpha$-pinene SOA particles are shown as orange, dotted lines. Homogeneous freezing conditions were calculated following Appendix B in Welti et al. (2020) and using the growth factor for $\alpha$-pinene SOA given in Varutbangkul et al. (2006).

formation of SOA particles with O:C ratios between 0.45 and 1.1, regardless of the oxidative age itself.

A strong dependence of ice formation on SOA water content was observed. Dry and super dry SOA particles (5) ($RH_W = 10\%$ and <1%, middle and right column in Fig. 2) form ice at humidities close to the homogeneous freezing line of solutes, the so-called Koop line (Koop et al., 2000), suggesting homogeneous freezing. Wet preconditioning of the SOA (at 40% $RH_W$, left column in Fig. 2) almost completely (10) suppressed the formation of ice up to water saturation. SOA particles preconditioned at higher $RH_W$ contain more water, which acts as a plasticizer, and they are therefore less viscous. It was expected that the higher water content of the particles would facilitate the diffusion of condensed water (15) molecules, enabling the homogeneous freezing of SOA solution droplets. To our knowledge, a retardation of homogeneous freezing of SOA particles with higher water content has not been observed experimentally and only recently been suggested by Fowler et al. (2020), based on simulations. Fig. (20) 4. illustrates the mechanism how water content could impact homogeneous freezing of SOA particles during SPIN measurements.

When dry SOA particles (Fig. 4a) take up water at low temperature inside SPIN, water diffusion towards the parti-
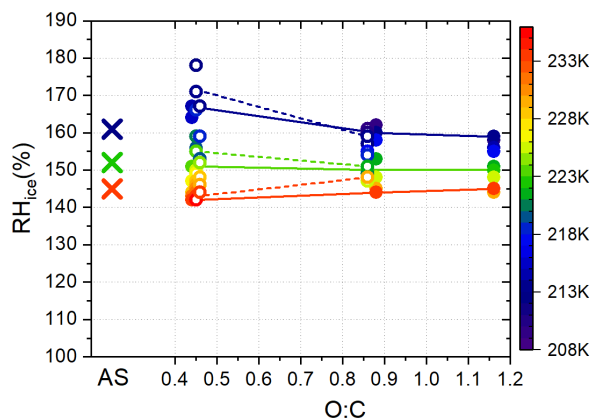
**Figure 3.** Relative humidity of ice formation on 1% of 100 nm $\alpha$-pinene SOA particles as function of O:C ratio (circles) in comparison to ammonium sulfate (AS, shown as crosses, data from Welti et al. (2020)). Open circles indicate experiments with $\alpha$-pinene particles preconditioned at $RH_W$<1%, filled circles $RH_W$=10%. Trendlines are shown for experiments at 213 K, 223 K and 233 K. Temperature is indicated by the color scale.

cle core is slow enough to enable the formation of a liquid (25)
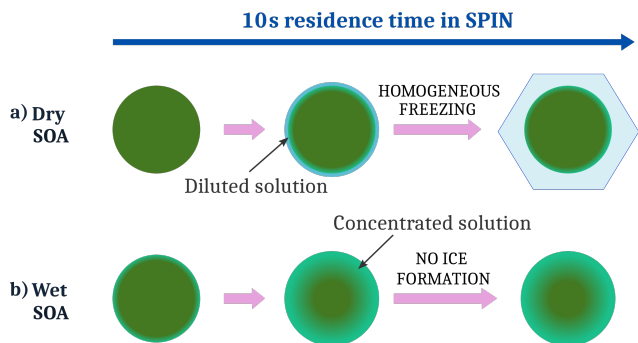
**Figure 4.** Suggested freezing mechanism for SOA particles with different water content.

**Figure 5.** Comparison of SOA pre-treatment conditions to SOA phase transition (viscosity $4{\times}10^5$ to $6{\times}10^6$ Pa s, red envelope) from Petters et al. (2019). We note that the phase transition coincides with a partial water vapor pressure (shown in blue) of 3-5 hPa. Homogeneous ice nucleation was only observed for SOA particles exposed to low water vapor pressure during pre-conditioning.

layer in equilibrium with SPIN conditions. This outer liquid layer in equilibrium with the surrounding RH freezes at the homogeneous freezing conditions (Koop et al., 2000). This mechanism is similar to the one suggested by Fowler et al. (2020).

For SOA particles with higher water content (Fig. 4b), water diffuses faster into the particle, removing water from the surface. Assuming a comparable amount of water taken up by the wet- and dry-conditioned SOA during their 10 s residence time in SPIN, wet-conditioned particles can not reach equilibrium, resulting in a more concentrated state, too concentrated to freeze homogeneously. Longer residence times could restore the homogeneous freezing of the particles by the equilibration with the surrounding RH. However, as equilibration time scales can be on the order of minutes and longer (Price et al., 2015), we believe that the observed inhibition of homogeneous freezing could also happen in fast updrafts in the atmosphere.

Comparing the preconditioning humidities to the phase diagram of RH-induced glass transition as a function of temperature for $\alpha$-pinene SOA in Fig. 5 (reproduced from Petters et al., 2019) suggests that SOA particles were in a liquid-like state before entering the SPIN instrument for the wet preconditioning (cross in Fig. 5, indicating suppression of ice formation). Dry preconditioned particles, for which homogeneous ice formation was observed, were likely glassy (blue hexagons in Fig. 5). The hygroscopic growth factors of $\alpha$-pinene SOA at 10% and 40% $RH_W$ are 1.00008, and 1.00718 (Varutbangkul et al., 2006). Assuming an average molecular weight of $200 \, \mathrm{g \, mol^{-1}}$ and a density of $1.5 \, \mathrm{g \, cm^{-3}}$ for the SOA particles, the corresponding water contents are 0.17% and 14% mole fractions, respectively. This indicates that at 40% $RH_W$ SOA particles can take up a substantial amount of water molecules. Evaporation studies on $\alpha$-pinene SOA (Li et al., 2019) also indicate that at room temperature and 40% $RH_W$ $\alpha$-pinene SOA particles present negligible kinetic limitations, evaporating in a nearly liquid-like state, while reduced $RH_W$ conditions (<1% $RH_W$) lead to slower evaporation rates, due to the limited bulk diffusivity of the particles. According to Fig. 5, once the SOA particles enter the SPIN

instrument, the particles solidify abruptly with the decreasing temperature, but seem to retain a preconditioning humidity dependent water diffusion rate, governing the equilibration timescale.

We propose that a partial water vapor pressure of 3-5 hPa can be used as marker condition to distinguish water diffusion rates of $\alpha$-pinene particles. Slower water diffusion into particles kept below 3-5 hPa leading to faster equilibration and homogeneous ice formation, while particles crossing this condition show faster diffusion and require longer equilibration times. To better understand the size dependent equilibration timescales of the wet or (super-) dry preconditioned particles and consequently the time dependence of homogeneous ice formation on SOA particles, additional experiments are needed. It would be beneficial to investigate in detail the correlation between the homogeneous ice nucleation ability of SOA and water content by extending the T-, and RH- conditions at which SOA are preconditioned to cover the threshold conditions shown in Fig. 5, including different particles sizes.

## 3.2 $\alpha$-pinene as proxy for boreal forest emissions

After isoprene, monoterpenes are the second most emitted volatiles by plants (Sindelarova et al., 2014). Among monoterpenes, $\alpha$-pinene is the most abundant VOC emitted from the boreal forest (Wang et al., 2018). We studied the ice nucleation conditions of SOA particles nucleated from Scots pine tree emissions and compared them to two precursor proxies: pine-needle oil (Sigma Aldrich) and $\alpha$-pinene. The SOA particles were generated in an ASC (Fig.1) and their IN ability tested between 210 K and 240 K and from ice
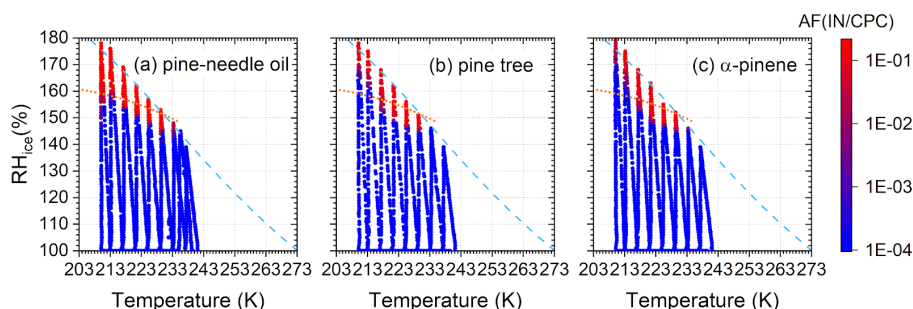
**Figure 6.** Activated fraction of 100 nm SOA particles. The precursor type is indicated in each subfigure. The light blue, dashed line marks water saturation. Conditions where 1% soluble particles freeze homogeneously according to the parameterization of Koop et al. (2000) are shown as orange curves, dotted lines.

to water saturation (Fig. 6). This is the first study measuring the IN ability of pure SOA from real pine emissions representative of boreal forest environments in laboratory controlled conditions.

5 The particles nucleated ice only at humidities close to the Koop line between approx. 215 K and 235 K, showing a steep onset when humidity increased during the RH-scans. Compared to the Koop parametrization, ice formation on Scots pine tree (Fig. 6b) and $\alpha$-pinene (Fig. 6c) SOA is re-
10 tarded to higher supersaturations in the lowest range of temperatures, similar to dry-conditioned $\alpha$-pinene SOA generated in the PAM reactor. In summary, the three tested precursors showed similar ice nucleation conditions, typical for homogeneous freezing, indicating that $\alpha$-pinene is an appro-
15 priate proxy for IN by SOA from boreal forests emissions.

### 3.3 Comparison to previous measurements of $\alpha$-pinene SOA ice formation conditions

The 1% AF values extracted from the RH- scans with dry and super dry $\alpha$-pinene SOA are summarized in Fig. 7 together
20 with data from the literature.

Conditions of 1% AF ice formation on $\alpha$-pinene SOA, measured in this study agree well with previous measurements reported by e.g. Ladino et al. (2014), Wagner et al. (2017), and Charnawskas et al. (2017). In these studies, SOA
25 particles were generated at T-, and RH-conditions comparable to the experiments for dry preconditioned SOA presented here. These studies concluded that $\alpha$-pinene SOA is a poor ice nucleating particle for heterogeneous ice formation or that they exclusively nucleate ice homogeneously. However,
30 the data deviates from the Koop line. Humidity conditions of ice formation decrease monotonically with increasing temperature, approximately parallel to the water saturation line, i.e. showing earlier onsets for the warmest temperatures and delayed onset at the cold temperatures. Ignatius et al. (2016)
35 argued that ice forming below the Koop line should be classified as heterogeneous ice formation. However, homogeneous ice formation below the Koop line was also observed during reference measurements using ammonium sulfate solu-
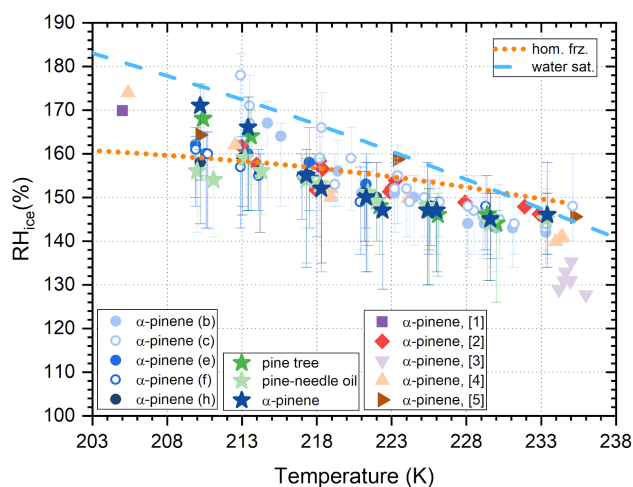
**Figure 7.** Conditions of ice formation on 1% of 100 nm $\alpha$-pinene SOA particles. Circles and stars represent the results from the PAM and ASC experiments, respectively. Open and filled symbols mark $RH_W$=1% and 10% preconditioning, respectively. $\alpha$-pinene SOA ice nucleation data from previous studies are shown for comparison: [1] Möhler et al. (2008), [2] Ladino et al. (2014), [3] Ignatius et al. (2016), [4] Wagner et al. (2017), [5] Charnawskas et al. (2017). The light blue dashed line marks water saturation. Conditions where 1% soluble particles freeze homogeneously according to the parameterization of Koop et al. (2000) are shown as dotted, orange curve.

tion droplets with the SPIN instrument (Welti et al., 2020). A steep increase in the AF at a certain humidity during RH- 40 scans is an additional indication that the driving ice formation mechanism was homogeneous freezing, despite the lower humidities for ice nucleation in comparison to the Koop parametrization.

Delayed onsets of homogeneous freezing above the hu- 45 midity defined by the water activity criterion (Koop et al., 2000) at low temperatures could indicate that particles are not in equilibrium before freezing in SPIN. A similar offset for homogeneous freezing of sulfuric acid particles at low temperature has been observed in the AIDA chamber (Möhler 50

et al., 2003), which was also attributed to diffusion-limited uptake of water vapor during cooling. The systematic delay of homogeneous freezing towards higher humidity, suggests a decreasing, low water diffusion rate of SOA towards low temperature. Fowler et al. (2020) pointed out the same aspect, and proposed even an inhibition of homogeneous ice nucleation below 200 K. Experimental evidence of homogeneous freezing inhibition at such low temperatures had been previously reported by Murray (2008) for citric acid solution droplets.

## 4   Conclusions

We have investigated the influence of particle water content and oxidative age on the ice nucleation ability of boreal forest SOA surrogates, using $\alpha$-pinene SOA generated in a PAM reactor as a model compound. The suitability of $\alpha$-pinene SOA as a proxy for the IN ability of more complex boreal forest surrogates was addressed by comparing IN measurements of SOA from two other precursors (pine-needle oil and Scots pine tree VOC) generated in an ASC under more atmospherically relevant conditions. For the first time, the IN ability of pure lab-generated SOA from real pine emission has been measured.

Boreal forest SOA surrogates from all precursors were found to be inefficient ice nucleating particles, in agreement with previous studies (e.g., Möhler et al., 2008; Ladino et al., 2014; Charnawskas et al., 2017). Our observations indicate that the IN ability of $\alpha$-pinene SOA can be considered representative of more complex SOA produced in monoterpene-dominated precursor mixes from boreal environments.

Homogeneous ice nucleation was observed for $\alpha$-pinene SOA preconditioned at low $RH_W$ ($\leq 10\%$) and contrary to the expected behavior, homogeneous freezing was suppressed for SOA with higher water content (40% $RH_W$). The onset humidity for homogeneous freezing did not depend on the oxidative age. The experiments indicate that SOA water content was the main variable controlling the onset humidity for homogeneous freezing at a certain temperature and point to a dependence on the water diffusion rate.

$\alpha$-pinene SOA with low water content, presumably in a highly viscous state, did not act as INP, but a decreased water diffusion rate into the particle allowed the formation of a core-shell morphology, enabling the homogeneous freezing of the diluted outer layer. In contrast, SOA with higher water content, into which water diffused more efficiently during the residence time in SPIN, completely liquefied or developed a core-shell morphology in which the liquid phase was highly concentrated, inhibiting homogeneous freezing. The coincidence of SOA phase transition conditions with partial water vapor pressures between 3-5 hPa also point at the potential dominant role of water content in particle properties like viscosity or diffusivity that affected the SOA ice nucleation behavior as measured by SPIN.

Further investigations should include SOA generation under a wider range of RH and T conditions and measurements of initial viscosity for a clearer connection between the ice nucleation measurements and the freezing pathways leading to those observations.

*Data availability.* Data sets are available from the authors upon request.

*Author contributions.* AV and AL proposed the initial research question. AAP and AW conducted the ice nucleation experiments with contributions from KK. AB, IP and IS were in charge of particle formation, characterization, and the corresponding data analysis. AAP and AW prepared the manuscript with contributions from AB, AL, and AV. All authors commented the manuscript. AV and AL acquired funding and supervised the project.

*Competing interests.* The authors declare that they have no conflict of interest.

*Acknowledgements.* We thank Zijun Li (Rex) and Pasi Miettinen for their support during the campaign. This work was supported by the Academy of Finland, C-Main project (grant no. 309141), and the Center of Excellence program (grant no. 307331).

## References

Bastelberger, S., Krieger, U. K., Luo, B. P., and Peter, T.: Time evolution of steep diffusion fronts in highly viscous aerosol particles measured with Mie resonance spectroscopy, J. Chem. Phys., 149, doi:10.1063/1.5052216, 2018.

Berkemeier, T., Shiraiwa, M., Pöschl, U., and Koop, T.: Competition between water uptake and ice nucleation by glassy organic aerosol particles, Atmos. Chem. Phys., 14, 12 513–12 531, doi:10.5194/acp-14-12513-2014, 2014.

Bertozzi, B., Wagner, R., Höhler, K., Pfeifer, J., Saathoff, H., Song, J., Leisner, T., and Möhler, O.: Ice nucleation ability of Ammonium Sulfate aerosol particles internally mixed with Secondary Organics, Atmos. Chem. Phys. Discuss., pp. 1–31, doi:10.5194/acp-2021-53, 2021.

Bond, T. C., Doherty, S. J., Fahey, D. W., Forster, P. M., Berntsen, T., DeAngelo, B. J., Flanner, M. G., Ghan, S., Kärcher, B., Koch, D., Kinne, S., Kondo, Y., Quinn, P. K., Sarofim, M. C., Schultz, M. G., Schulz, M., Venkataraman, C., Zhang, H., Zhang, S., Bellouin, N., Guttikunda, S. K., Hopke, P. K., Jacobson, M. Z., Kaiser, J. W., Klimont, Z., Lohmann, U., Schwarz, J. P., Shindell, D., Storelvmo, T., Warren, S. G., and Zender, C. S.: Bounding the role of black carbon in the climate system: A scientific assessment, J. Geophys. Res. Atmos., 118, 5380–5552, doi:10.1002/jgrd.50171, 2013.

Charnawskas, J. C., Alpert, P. A., Lambe, A. T., Berkemeier, T., O'Brien, R. E., Massoli, P., Onasch, T. B., Shiraiwa, M., Moffet, R. C., Gilles, M. K., Davidovits, P., Worsnop, D. R., and Knopf, D. A.: Condensed-phase biogenic–anthropogenic inter-

actions with implications for cold cloud formation, Faraday Discuss., 200, 165–194, doi:10.1039/C7FD00010C, 2017.

Cziczo, D. J., Froyd, K. D., Hoose, C., Jensen, E. J., Diao, M., Zondlo, M. A., Smith, J. B., Twohy, C. H., and Murphy, D. M.: Clarifying the Dominant Sources and Mechanisms of Cirrus Cloud Formation, Science, 340, 1320–1324, doi:10.1126/science.1234145, 2013.

DeCarlo, P. F., Kimmel, J. R., Trimborn, A., Northway, M. J., Jayne, J. T., Aiken, A. C., Gonin, M., Fuhrer, K., Horvath, T., Docherty, K. S., Worsnop, D. R., and Jimenez, J. L.: Field-Deployable, High-Resolution, Time-of-Flight Aerosol Mass Spectrometer, Anal. Chem., 78, 8281–8289, doi:8410.1029/2001JD001213.Analytical, 2006.

DeMott, P. J., Cziczo, D. J., Prenni, A. J., Murphy, D. M., Kreidenweis, S. M., Thomson, D. S., Borys, R., and Rogers, D. C.: Measurements of the concentration and composition of nuclei for cirrus formation, P. Natl. Acad. Sci. USA, 100, 14 655–14 660, doi:10.1073/pnas.2532677100, 2003.

Faiola, C. L., Pullinen, I., Buchholz, A., Khalaj, F., Ylisirniö, A., Kari, E., Miettinen, P., Holopainen, J. K., Kivimäenpää, M., Schobesberger, S., Yli-Juuti, T., and Virtanen, A.: Secondary Organic Aerosol Formation from Healthy and Aphid-Stressed Scots Pine Emissions, ACS Earth Space Chem., 3, 1756–1772, doi:10.1021/acsearthspacechem.9b00118, 2019.

Fowler, K., Connolly, P., and Topping, D.: Modelling the effect of condensed-phase diffusion on the homogeneous nucleation of ice in ultra-viscous particles, Atmos. Chem. Phys., 20, 683–698, doi:10.5194/acp-20-683-2020, 2020.

Garimella, S., Kristensen, T. B., Ignatius, K., Welti, A., Voigtländer, J., Kulkarni, G. R., Sagan, F., Kok, G. L., Dorsey, J., Nichman, L., Rothenberg, D. A., Rösch, M., Kirchgäßner, A. C. R., Ladkin, R., Wex, H., Wilson, T. W., Ladino, L. A., Abbatt, J. P. D., Stetzer, O., Lohmann, U., Stratmann, F., and Cziczo, D. J.: The SPectrometer for Ice Nuclei (SPIN): an instrument to investigate ice nucleation, Atmos. Meas. Tech., 9, 2781–2795, doi:10.5194/amt-9-2781-2016, 2016.

Ignatius, K., Kristensen, T. B., Järvinen, E., Nichman, L., Fuchs, C., Gordon, H., Herenz, P., Hoyle, C. R., Duplissy, J., Garimella, S., Dias, A., Frege, C., Höppel, N., Tröstl, J., Wagner, R., Yan, C., Amorim, A., Baltensperger, U., Curtius, J., Donahue, N. M., Gallagher, M. W., Kirkby, J., Kulmala, M., Möhler, O., Saathoff, H., Schnaiter, M., Tomé, A., Virtanen, A., Worsnop, D., and Stratmann, F.: Heterogeneous ice nucleation of viscous secondary organic aerosol produced from ozonolysis of α-pinene, Atmos. Chem. Phys, 16, 6495–6509, doi:10.5194/acp-16-6495-2016, 2016.

Kang, E., Root, M. J., Toohey, D. W., and Brune, W. H.: Introducing the concept of Potential Aerosol Mass (PAM), Atmos. Chem. Phys, 7, 5727–5744, doi:10.5194/acp-7-5727-2007, 2007.

Knopf, D. A., Alpert, P. A., and Wang, B.: The Role of Organic Aerosol in Atmospheric Ice Nucleation: A Review, ACS Earth Space Chem., 2, 168–202, doi:10.1021/acsearthspacechem.7b00120, 2018.

Koop, T., Luo, B., Tsias, A., and Peter, T.: Water activity as the determinant for homogeneous ice nucleation in aqueous solutions, Nature, 406, 611–614, doi:10.1038/35020537, 2000.

Koop, T., Bookhold, J., Shiraiwa, M., and Pöschl, U.: Glass transition and phase state of organic compounds: dependency on molecular properties and implications for secondary organic

aerosols in the atmosphere, Phys. Chem. Chem. Phys., 13, 19 238, doi:10.1039/c1cp22617g, 2011.

Ladino, L. A., Zhou, S., Yakobi-Hancock, J. D., Aljawhary, D., and Abbatt, J. P. D.: Factors controlling the ice nucleating abilities of α-pinene SOA particles, J. Geophys. Res. Atmos., 119, 9041–9051, doi:10.1002/2014JD021578, 2014.

Lambe, A. T., Ahern, A. T., Williams, L. R., Slowik, J. G., Wong, J. P. S., Abbatt, J. P. D., Brune, W. H., Ng, N. L., Wright, J. P., Croasdale, D. R., Worsnop, D. R., Davidovits, P., and Onasch, T. B.: Characterization of aerosol photooxidation flow reactors: heterogeneous oxidation, secondary organic aerosol formation and cloud condensation nuclei activity measurements, Atmos. Meas. Tech., 4, 445–461, doi:10.5194/amt-4-445-2011, 2011.

Li, Z., Tikkanen, O. P., Buchholz, A., Hao, L., Kari, E., Yli-Juuti, T., and Virtanen, A.: Effect of Decreased Temperature on the Evaporation of α-Pinene Secondary Organic Aerosol Particles, ACS Earth Space Chem., 3, 2775–2785, doi:10.1021/acsearthspacechem.9b00240, 2019.

Lienhard, D. M., Huisman, A. J., Krieger, U. K., Rudich, Y., Marcolli, C., Luo, B. P., Bones, D. L., Reid, J. P., Lambe, A. T., Canagaratna, M. R., Davidovits, P., Onasch, T. B., Worsnop, D. R., Steimer, S. S., Koop, T., and Peter, T.: Viscous organic aerosol particles in the upper troposphere: diffusivity-controlled water uptake and ice nucleation?, Atmos. Chem. Phys., 15, 13 599–13 613, doi:10.5194/acp-15-13599-2015, 2015.

Mikhailov, E., Vlasenko, S., Martin, S. T., Koop, T., and Pöschl, U.: Amorphous and crystalline aerosol particles interacting with water vapor: conceptual framework and experimental evidence for restructuring, phase transitions and kinetic limitations, Atmos. Chem. Phys., 9, 9491–9522, doi:10.5194/acp-9-9491-2009, 2009.

Möhler, O., Stetzer, O., Schaefers, S., Linke, C., Schnaiter, M., Tiede, R., Saathoff, H., Krämer, M., Mangold, A., Budz, P., Zink, P., Schreiner, J., Mauersberger, K., Haag, W., Kärcher, B., and Schurath, U.: Experimental investigation of homogeneous freezing of sulphuric acid particles in the aerosol chamber AIDA, Atmos. Chem. Phys., 3, 211–223, doi:10.5194/acp-3-211-2003, 2003.

Möhler, O., Benz, S., Saathoff, H., Schnaiter, M., Wagner, R., Schneider, J., Walter, S., Ebert, V., and Wagner, S.: The effect of organic coating on the heterogeneous ice nucleation efficiency of mineral dust aerosols, Environ. Res. Lett., 3, 025 007, doi:10.1088/1748-9326/3/2/025007, 2008.

Murray, B. J.: Inhibition of ice crystallisation in highly viscous aqueous organic acid droplets, Atmos. Chem. Phys., 8, 5423–5433, doi:10.5194/acp-8-5423-2008, 2008.

Murray, B. J., Wilson, T. W., Dobbie, S., Cui, Z., Al-Jumur, S. M. R. K., Möhler, O., Schnaiter, M., Wagner, R., Benz, S., Niemand, M., Saathoff, H., Ebert, V., Wagner, S., and Kärcher, B.: Heterogeneous nucleation of ice particles on glassy aerosols under cirrus conditions, Nat. Geosci., 3, 233–237, doi:10.1038/ngeo817, 2010.

Peng, Z., Day, D. A., Stark, H., Li, R., Lee-Taylor, J., Palm, B. B., Brune, W. H., and Jimenez, J. L.: HOx radical chemistry in oxidation flow reactors with low-pressure mercury lamps systematically examined by modeling, Atmos. Meas. Tech., 8, 4863–4890, doi:10.5194/amt-8-4863-2015, 2015.

Petters, S. S., Kreidenweis, S. M., Grieshop, A. P., Ziemann, P. J., and Petters, M. D.: Temperature- and Humidity-Dependent

Phase States of Secondary Organic Aerosols, Geophys. Res. Lett., 46, 1005–1013, doi:10.1029/2018GL080563, 2019.

Prenni, A. J., Petters, M. D., Faulhaber, A., Carrico, C. M., Ziemann, P. J., Kreidenweis, S. M., and DeMott, P. J.: Heterogeneous ice nucleation measurements of secondary organic aerosol generated from ozonolysis of alkenes, Geophys. Res. Lett., 36, L06 808, doi:10.1029/2008GL036957, 2009.

Price, H. C., Mattsson, J., Zhang, Y., Bertram, A. K., Davies, J. F., Grayson, J. W., Martin, S. T., O'Sullivan, D., Reid, J. P., Rickards, A. M. J., and Murray, B. J.: Water diffusion in atmospherically relevant $\alpha$-pinene secondary organic material, Chem. Sci., 6, 4876–4883, doi:10.1039/C5SC00685F, 2015.

Schill, G. P. and Tolbert, M. A.: Depositional ice nucleation on monocarboxylic acids: Effect of the O:C ratio, Journal of Physical Chemistry A, 116, 6817–6822, doi:10.1021/jp301772q, 2012.

Schill, G. P., De Haan, D. O., and Tolbert, M. A.: Heterogeneous Ice Nucleation on Simulated Secondary Organic Aerosol, Environ. Sci. Technol., 48, 1675–1682, doi:10.1021/es4046428, 2014.

Shiraiwa, M., Yee, L. D., Schilling, K. A., Loza, C. L., Craven, J. S., Zuend, A., Ziemann, P. J., and Seinfeld, J. H.: Size distribution dynamics reveal particle-phase chemistry in organic aerosol formation, P. Natl. Acad. Sci. USA, 110, 11 746–11 750, doi:10.1073/pnas.1307501110, 2013.

Sindelarova, K., Granier, C., Bouarar, I., Guenther, A., Tilmes, S., Stavrakou, T., Müller, J.-F., Kuhn, U., Stefani, P., and Knorr, W.: Global data set of biogenic VOC emissions calculated by the MEGAN model over the last 30 years, Atmos. Chem. Phys., 14, 9317–9341, doi:10.5194/acp-14-9317-2014, 2014.

Varutbangkul, V., Brechtel, F. J., Bahreini, R., Ng, N. L., Keywood, M. D., Kroll, J. H., Flagan, R. C., Seinfeld, J. H., Lee, A., and Goldstein, A. H.: Hygroscopicity of secondary organic aerosols formed by oxidation of cycloalkenes, monoterpenes, sesquiterpenes, and related compounds, Atmos. Chem. Phys., 6, 2367–2388, doi:10.5194/acp-6-2367-2006, 2006.

Virtanen, A., Joutsensaari, J., Koop, T., Kannosto, J., Yli-Pirilä, P., Leskinen, J., Mäkelä, J. M., Holopainen, J. K., Pöschl, U., Kulmala, M., Worsnop, D. R., and Laaksonen, A.: An amorphous solid state of biogenic secondary organic aerosol particles, Nature, 467, 824–827, doi:10.1038/nature09455, 2010.

Wagner, R., Höhler, K., Huang, W., Kiselev, A., Möhler, O., Mohr, C., Pajunoja, A., Saathoff, H., Schiebel, T., Shen, X., and Virtanen, A.: Heterogeneous ice nucleation of $\alpha$-pinene SOA particles before and after ice cloud processing, J. Geophys. Res. Atmos., 122, 4924–4943, doi:10.1002/2016JD026401, 2017.

Wang, B., Lambe, A. T., Massoli, P., Onasch, T. B., Davidovits, P., Worsnop, D. R., and Knopf, D. A.: The deposition ice nucleation and immersion freezing potential of amorphous secondary organic aerosol: Pathways for ice and mixed-phase cloud formation, J. Geophys. Res. Atmos., 117, doi:10.1029/2012JD018063, 2012.

Wang, M., Schurgers, G., Hellén, H., Lagergren, F., and Holst, T.: Biogenic volatile organic compound emissions from a boreal forest floor, Boreal Environ. Res., 23, 249–265, http://www.borenv.net/BER/archive/pdfs/ber23/ber23-249-265.pdf, 2018.

Welti, A., Korhonen, K., Miettinen, P., Piedehierro, A. A., Viisanen, Y., Virtanen, A., and Laaksonen, A.: SPIN modification for low-temperature experiments, Atmos. Meas. Tech., 13, 7059–7067, doi:10.5194/amt-13-7059-2020, 2020.

Wolf, M. J., Zhang, Y., Zawadowicz, M. A., Goodell, M., Froyd, K., Freney, E., Sellegri, K., Rösch, M., Cui, T., Winter, M., Lacher, L., Axisa, D., DeMott, P. J., Levin, E. J., Gute, E., Abbatt, J., Koss, A., Kroll, J. H., Surratt, J. D., and Cziczo, D. J.: A biogenic secondary organic aerosol source of cirrus ice nucleating particles, Nat. Commun., 11, doi:10.1038/s41467-020-18424-6, 2020.

Yli-Juuti, T., Pajunoja, A., Tikkanen, O., Buchholz, A., Faiola, C., Väisänen, O., Hao, L., Kari, E., Peräkylä, O., Garmash, O., Shiraiwa, M., Ehn, M., Lehtinen, K., and Virtanen, A.: Factors controlling the evaporation of secondary organic aerosol from $\alpha$-pinene ozonolysis, Geophys. Res. Lett., 44, 2562–2570, doi:10.1002/2016GL072364, 2017.

Zobrist, B., Marcolli, C., Pedernera, D. A., and Koop, T.: Do atmospheric aerosols form glasses?, Atmos. Chem. Phys., 8, 5221–5244, doi:10.5194/acp-8-5221-2008, 2008.